

Preparation of NiMn₂O₄-NiMnO₃@MoS₂ Nano-composites with Enhanced Electrochemical Performances for Lithium-ion Batteries

Anchali Jain, Amrish K Panwar*, & Pawan K Tyagi

Department of Applied Physics, Delhi Technological University, New Delhi 110 042, India

Received: 9 August 2023; Accepted: 26 September 2023

With the technological development in rechargeable lithium-ion batteries (LIBs), there have been a requirement for advanced anodes to complete the demand of energy storage devices. Among the developed anode, Mixed Transition Metal Oxides (MTMOs) are one of the evolving categories. MTMOs provide a synergistic effect due to the presence of multiple elements which enhance the electrochemical performance. Similarly, 2D MoS₂ have been an emerging anode for Lithium-ion Batteries. Therefore, in this work, the preparation of NiMn₂O₄-NiMnO₃@MoS₂(NMO-MoS₂) nano-composites have been attempted. Structural, microstructural and other physicochemical characterization have been investigated by X-ray diffraction, Scanning Electron Microscopy. Electrochemical characterizations also analyzed via Cyclic Voltammetry, Electrochemical Impedance Spectroscopy, and Galvanostatic Charge-Discharge analysis. In the MoS₂ type of composite, the layered structure of MoS₂ provides intercalation of lithium ions without any major volume expansion of NiMn₂O₄-NiMnO₃ (NMO) material. Furthermore, NMO nanoparticles occupy the spaces between the MoS₂ nanosheets making both faces accessible to electrolyte penetration. The resulting composite material displayed a stable cyclic voltammogram profile and discharge capacity of 361.54 mAhg⁻¹ even after 200 cycles at the current density of 500mA g⁻¹.

Keywords: Composite, Lithium-ion Batteries, MoS₂, NiMn₂O₄, NiMnO₃

1 Introduction

In recent years, lithium-ion battery technologies have been evolving very rapidly, demanding the development and innovations in electrode materials in terms of higher energy density, longer cycle life, and advanced electrochemical stability. In general, commercialized anode graphite has been used due to its abundance, low cost, and advantageous hexagonal stacked structure for Li-ion insertion.¹ But its shortcomings such as low theoretical capacity (~372 mAh g⁻¹), decreasing rate capability, and low working potential results in dendrites formation on the surface resulting in safety concerns that limit its practical use.¹ Contrary, conversion mechanism-based transition metal oxides (TMOs) show potential towards Lithium-ion batteries (LIBs), attaining high capacities (700-1200 mAh g⁻¹).² Among the other TMOs, Mn-based and Ni-based oxides have been much explored because of their superior theoretical capacities, low lithiation potential (~0.4V), and cost-effectiveness.³⁻⁴ Furthermore, mixed metal oxides such as NiMn₂O₄ (Nickel-Manganese Oxide) attain better electrochemistry compared to single metal oxides due to the synergistic effect between the multiple oxidation states.⁴ However, its disadvantages

such as poor conductivity and volume expansion, result in capacity fading and poor rate performances occur.³⁻⁴ One way to solve these difficulties is to synthesize nano-sized structures which can provide increased surface area for the insertion of Li⁺ and lessen the diffusion path of Li⁺.² Another solution is to make a composite with other conductive materials.²

MoS₂ which has attained attention due to its 2D-layered structure, with unique electrochemical properties has been used as an anode for LIBs. Its layered structure can provide more space for Li⁺ insertion, and its high theoretical capacity makes it an ideal candidate for the composite.⁵⁻⁶ However, the aggregation and re-stacking of MoS₂ nano-sheets compromised its rate capability.⁷ Thus, new and innovative composite materials should be studied to overcome the limitations of materials.

Therefore, the designing of NiMn₂O₄-MoS₂ composite electrodes resolves the single material shortcomings in terms of stability, cyclability, and rate performance. NiMn₂O₄ (NMO) nanoparticles between the MoS₂ sheets suppress the volume expansion of NMO and solve the issues regarding the restacking in MoS₂.

Herein, we synthesized NiMn₂O₄-NiMnO₃@MoS₂ nano-composite using the facile and low-cost two-step strategy. The composite structural,

*Corresponding author (E-mail: amrish.phy@dtu.ac.in)

morphological, and electrochemical performance are studied. The prepared composite exhibit improved and stable cycle life. Thus, multiple active sites and the synergistic effect of both materials are responsible for the improved performance of the LIB anode.

2 Materials & Methods

2.1 Preparation of NiMn₂O₄ nanoparticles

The precursors of Ni(CH₃CO₂)₂·4H₂O and Mn(CH₃CO₂)₂·2H₂O were used to prepare. The chelating agent, citric acid, C₆H₈O₇ ratio was used as 1:1 with metal ions. After that, the high-energy ball mill was used for 4h at 300rpm to grind the precursors into light green-colored as-prepared samples. To remove any moisture content drying was done at 80°C. Black-colored NiMn₂O₄ was obtained after the calcination at 700°C under the air atmosphere, named NMO-bare was used further to make the composite.

2.2 Preparation of MoS₂ nanosheets

To prepare MoS₂, a facile and simple one-step hydrothermal method was used. Sodium Molybdate (Na₂MoO₄), and Thiourea (CH₄N₂S) were separately dissolved in DI (30ml) and mixed for 30mins. After that, homogeneous mixing was performed for 1hr. The prepared solution was treated at 200°C for 24hrs in a Teflon-lined hydrothermal autoclave. When the temperature cooled down, the collected black precipitate was washed several times with DI and ethanol. Further, to remove solvent it was dried at 80°C. The black sample was used for subsequent experiments.

2.3 Preparation of NiMn₂O₄-NiMnO₃@MoS₂ Composite

Firstly, MoS₂ suspension was ultrasonically mixed with ethanol as solvent. The MoS₂ solution was aged and after aging, NMO-bare nanoparticles were mixed and dried at 80°C. When the solution remains a little, it was dried at 80°C overnight. The black-colored sample was grinded, and collected for testing as an anode without any further modifications.

2.4 Characterizations

To study the phase and crystallinity of the final composites X-ray Diffraction (XRD) was performed via Rigaku X-ray diffractometer (Model: K-alpha). Morphological studies namely Scanning Electron Microscopy (SEM), and Energy-Dispersive X-ray Spectroscopy (EDX) were performed using Nova Nano Scanning Electron Microscope. Active material, carbon black, and binder polyvinylidene (PVDF) in

70:20:10 ratio were used to prepare anode electrodes for bare and composite samples. N-methyl pyrrolidone (NMP), Li metal, polypropylene sheet Celgard 2400, and 1M LiPF₆ in EC:DMC (1:1, by volume) were used as solvent, reference electrode, separator, and electrolyte respectively. All the electrodes prepared and coin-cell assembly fabrication and specifications were reported in the report.⁸ Cell testing on the freshly prepared cells was done using a biologic make VMP3 workstation. Electrochemical Impedance Spectroscopy (EIS) was investigated using a 5mV AC signal within the frequency range of 0.1MHz – 10mHz. Cyclic Voltammetry (CV) curves were recorded in the 0.01-3.0V potential window with 0.1mV/s scan rate. Neware make Battery Testing System (Model: BTS software 8.0) was used to study the Galvanostatic charge-discharge (GCD) profiles at varied current rates.

3 Results and Discussions

3.1 Phase analysis

Figure 1 displays the recorded XRD pattern of NiMn₂O₄-NiMnO₃@MoS₂ at room temperature. For comparison, NiMn₂O₄ (NMO-bare) and MoS₂ data are also displayed. All the peaks of composite and bare samples were sharp in nature, it reveals the crystalline nature of the materials. NMO-bare diffracted peaks were well indexed to JCPDS no. 01-074-1865, acquiring cubic structure with Fd3m space group. Similarly, MoS₂ diffracted peaks depict the formation of a hexagonal structure with a P6₃mmc space group (JCPDS no. 00-037-1492).

However, after the treatment with MoS₂ suspension, the composite consists of diffracted peaks

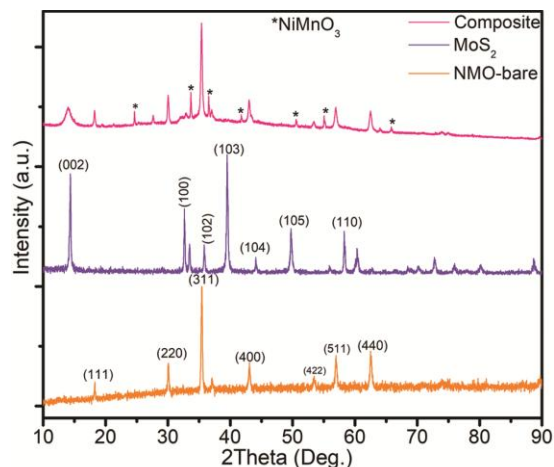


Fig. 1 — XRD pattern of NiMn₂O₄-NiMnO₃@MoS₂ composite recorded from 10 to 90°.

of NMO with a slight presence of rhombohedral NiMnO_3 phase (JCPDS no. 01-075-2089). Furthermore, a broad peak of MoS_2 at 14.14° corresponds to the (002) plane confirming the hybrid formation of phase. Thus, the formed composite depicts a crystalline structure that maybe advantageous for Li^+ and e^- transportation by providing a short length between the nanoparticles and nano-sheets.⁹

3.2 Morphological analysis

The prepared samples morphology were studied using Scanning Electron Microscopy (SEM) at varied magnifications as shown in Fig. 2(a-d). Figure 2(a) confirms the formation of MoS_2 nanosheets with slight

agglomeration. These nanosheets were structured together to form nanoflowers. Figure 2(b) shows the formation of NiMn_2O_4 (NMO) nanoparticles with particle size $<100\text{nm}$. It can be observed that the particles were lengthened and agglomerated due to the synthesis route used. Figure 2(c-d) displays the composite micrographs at two different magnifications. NMO nanoparticles and MoS_2 sheets were embedded together which could be due to the continuous mixing.

Elemental composition is validated via Energy-Dispersive X-ray Spectroscopy (EDX), shown in Fig. 3. From Fig. 3 (a-f), it is believed that the composite was uniformly formed which is consistent

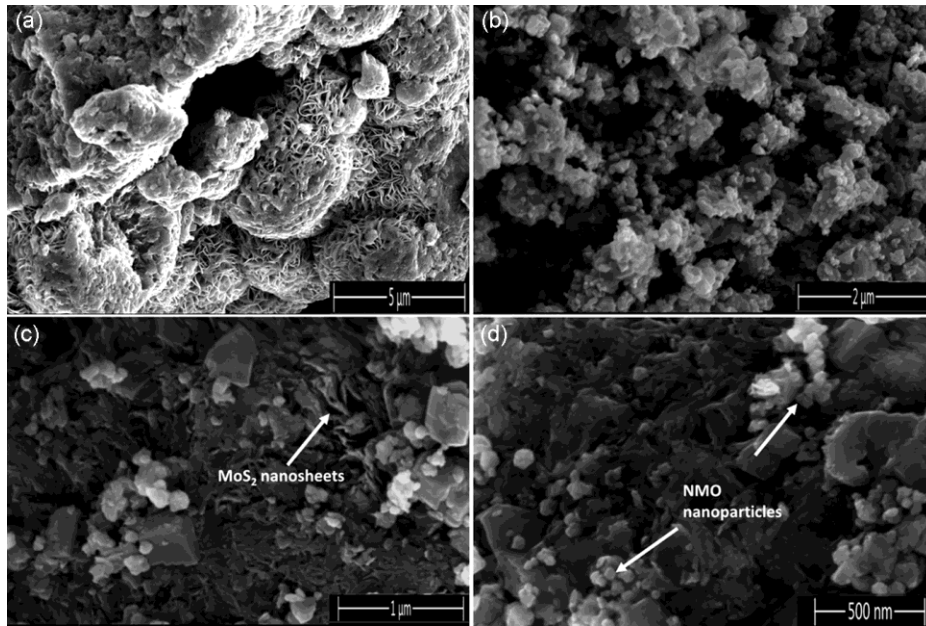


Fig. 2 — SEM images of (a) MoS_2 Nano-sheets, (b) Bare NiMn_2O_4 , & (c) $\text{NiMn}_2\text{O}_4\text{-NiMnO}_3\text{@MoS}_2$ composite recorded at different magnifications.

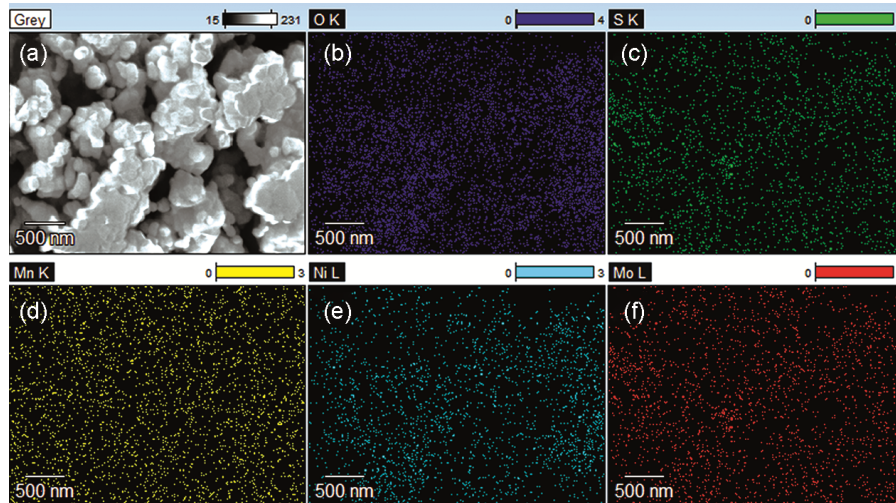


Fig. 3 — EDX mapping of $\text{NiMn}_2\text{O}_4\text{-NiMnO}_3\text{@MoS}_2$ composite recorded at room temperature.

with XRD results. The occurrence of elements, Ni, Mn, O, Mo, and S confirms the formation of the $\text{NiMn}_2\text{O}_4\text{-NiMnO}_3\text{@MoS}_2$ composite. From SEM and EDX results, it can be concluded that the formation of an NMO-MoS₂ composite with a unique structure may help in improving the electrochemical performance as an anode.

3.3 Electrochemical analysis

CV, and GCD profiles were used to examine the electrochemical properties as anode. Figures 4(a) and (b) show the CV curves of 1st and 3rd cycle recorded in the potential window of 0.01-3.0 V at 0.1 mV s⁻¹ scan rate respectively. During the charging and discharging process, multiple broad peaks of NiMn_2O_4 as well as MoS_2 can be observed in Fig. 4 (a-b) which shows the redox reaction of the unique composite structure. The dominant reduction peak at ~0.5V in both cycles depicts the reduction of Ni^{2+} and Mn^{3+} to metallic Ni and Mn respectively.¹⁰ In the third cycle, the strong peak at ~0.96V, attributes the reduction of Mn^{3+} to Mn^{2+} , while small peak at ~1.8V leads to the intercalation of Li^+ into MoS_2 and make it Li_2S phase.¹¹⁻¹² The broad oxidation peaks at ~1.9V, ~1.3V, and ~2.3V corresponds to the oxidation of Ni, Mn, and de-intercalation of Li^+ from Li_2S respectively.¹⁰⁻¹¹ Furthermore, with the increased

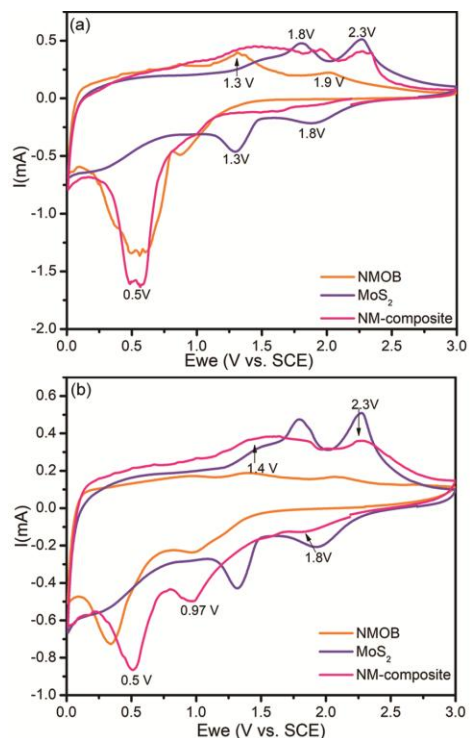


Fig. 4 — (a) Cycle 1st, (b) Cycle 3rd of cyclic CVs recorded at 0.1 mV s⁻¹ scan rate within the voltage window of 0.01-3.0V.

value of current from 3rd cycle, it is evident that the composite shows improved electrochemical performance than a single NiMn_2O_4 anode.

To study the Li^+ storage behavior, GCD was also attempted on the freshly made composite electrodes. Figure 5(a-b) shows the GCD profiles of the composite for the 1st, 2nd, 10th, and 20th cycles with corresponding dQ/dV curves at a high 500 mA g⁻¹ current density. The discharge voltage plateaus and reduction/oxidation peaks are consistent with CV curves, indicating the electrochemical reactions between NiMn_2O_4 , MoS_2 , and Li^+ . From Fig. 5(a-b), three discharge plateaus with corresponding reduction peaks exist at ~1.7, ~1.0, and ~0.5V further validating that both the active materials i.e., NiMn_2O_4 and MoS_2 were involved in the electrochemical kinetics. The composite's 1st, 2nd, 10th, and 20th discharge capacities were 1074.36, 1010.35, 734.28, and 517.75 mAh g⁻¹ at a current density of 500 mA g⁻¹ respectively. Figure 5(c) displays the cycling performance of composite and bare NMO for 300 cycles recorded at 500 mA g⁻¹ current density. The composite structure attains discharge capacity of 306.42 mAh g⁻¹ even after 300 cycles at such a high current rate. However, in comparison bare NMO delivers 246.29 mAh g⁻¹ discharge capacity which depicts an improved electrochemical performance. This increment in the capacity could be due to the presence of NMO nanoparticles between the spaces of MoS_2 nanosheets and making both faces accessible to electrolyte penetration. Furthermore, MoS_2 nanosheets suppress

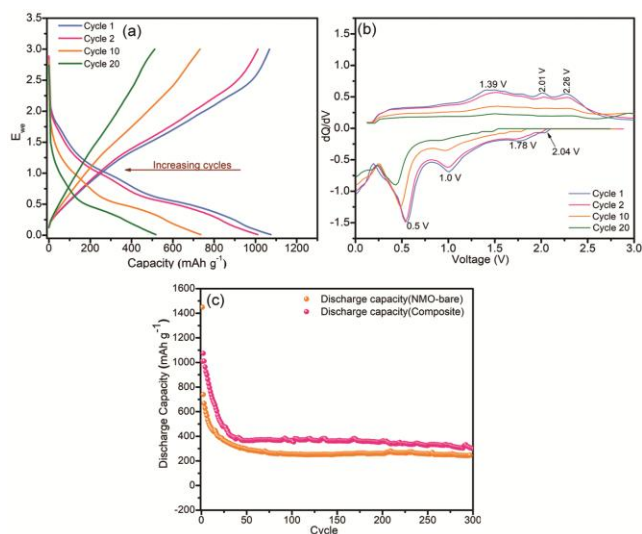


Fig. 5 — (a) Charge-discharge profiles of 1st, 2nd, 10th, and 20th cycles, (b) corresponding dQ/dV curves, & (c) cycle performance for 300 cycles recorded at 500 mA g⁻¹ current density in the potential window of 0.01-3.0V.

the volume expansion of NMO nanoparticles due to which it can attain stable cycling performance.

4 Conclusion

In summary, we have synthesized NiMn₂O₄-NiMnO₃@MoS₂ composites using a two-step method and studied their electrochemical performance as an alternative anode material. The unique composite formation with Fd3m, P6₃mmc, and rhombohedral space groups is confirmed using XRD analysis. Morphological studies confirm the NMO nanoparticles embedded in the MoS₂ nanosheets, however, the slight agglomeration could be seen due to the constant mixing. This unique structure facilitates the Li⁺ more effectively and provides more surface area for electrolyte penetration. CV multiple oxidation-reduction peaks at ~2.3V, ~1.8V, ~0.5V consistent with GCD curves confirm the excellent electrochemical performances of composite which is due to the synergistic effect of both materials.

Acknowledgment

This researchwork was sponsored by the project (F. No. DTU/IRD/619/2019/2114) granted to the Lithium-ion Battery Technology (LIBT) Lab,

Department of Applied Physics, Delhi Technological University (DTU), New Delhi.

References

- 1 Nzereogu P U, Omah A D, Ezema F I, Iwuoha E I & Nwanya A C, *Appl Surf Sci*, 9(2022) 100233.
- 2 Zhu J, Ding Y, Ma Z, Tang W, Chen X & Lu Y, *J Electron Mater*, 51 (2022) 3391.
- 3 Huang J, Wang W, Lin X, Gu C & Liu J, *J Power Sources*, 378 (2018) 677.
- 4 Sanchez J S, Pendashteh A, Jesus P, Marc A & Marcilla R, *Appl Surf Sci*, 460 (2018) 74.
- 5 Wang X, Zhang Z, Chen Y, Qu Y, Lai Y & Li J, *J Alloys Compd*, 600 (2014) 84.
- 6 Tian Y, Liu X, Cao X, Zhang D, Xiao S, Li X, Le Z, Li X & Li H, *Chem Eng J*, 374 (2019) 42.
- 7 Chen Y, Lu J, Wen S, Lu L & Xue J, *J Mater Chem A*, 2 (2014) 17857.
- 8 Jain A, Panwar A K, Tyagi P K, *MRS Advances*, 7 (2022) 584.
- 9 Lu F, Xu C, Meng F, Xia T, Wang R & Wang J, *Adv Mater Interfaces*, (2017) 1700639.
- 10 Ding L, Zheng X, Qin R, Guo P, Jiang X & Zeng M, *Mater Lett*, 323 (2022) 132561.
- 11 Rajoba S J, Kale R D, Kulkarni S B, Parale V G, Patil R, Olin H, Park H H, Dhavale R P & Phadatare M, *J compos sci*, 5 (2021) 69.
- 12 Sun P, Zhang W, Hu X, Yuan L & Huang Y, *J Mater Chem A*, 2 (2014) 3498.